

Compact RF Large-Signal Model for MEMS Capacitive Switches

Subrata Halder, Cristiano Palego, and James C. M. Hwang
Lehigh University, Bethlehem, PA 18103 USA

Charles L. Goldsmith
MEMtronics Corporation, Plano, TX 75075 USA

Abstract — Last year, we reported on a SPICE-based compact RF *small-signal electromechanical* model for electrostatically actuated MEMS capacitive shunt switches with movable membranes. We now report on the enhancement of the model to include *electrothermal* and *thermomechanical* effects so that the model is applicable under *large-signal* RF conditions. Specifically, a thermal subcircuit is added to account for the temperature rise in the switch membrane as a function of the dissipated RF power. In turn, the temperature rise is used to evaluate the decrease in the membrane spring constant. These enhancements allow the present multiphysics model to simulate the coupled self-biasing and self-heating effects under RF large signals and to predict the power-handling capacity of MEMS capacitive switches. Additionally, the model has been coded in Verilog, making it portable between different circuit simulation environments.

Index Terms — Capacitance measurement, electromechanical effects, microelectromechanical devices, microwave devices, microwave measurements, microwave switches.

I. INTRODUCTION

Similar to transistors in integrated circuits, switches are the basic building blocks of RF MEMS. As RF MEMS technology matures [1], increasing attention is focused on adaptive control and large-scale integration that require compact switch models to be available through popular circuit simulation environments. Currently, most RF MEMS switch models are either too complicated [2]-[8] to be implemented in popular circuit simulation environments or not complicated enough [9]-[13] to account for the switching transients between pull-in, contact, and release processes. Last year, we reported [14] on a SPICE-based compact RF *small-signal electromechanical* model for electrostatically actuated MEMS capacitive shunt switches, which can smoothly simulate the transients between pull-in, contact, and release. We now report on a compact RF *large-signal multiphysics* model, which can account for the coupled self-biasing and self-heating effects [15] as described below.

II. COMPACT MULTIPHYSICS MODEL

Fig. 1 shows the equivalent circuit of the kinetics of the movable membrane of an electrostatically actuated RF MEMS capacitive shunt switch with mass m , spring constant k , and damping factor b as governed by the following equation:

$$L'(\partial^2 V'/\partial t^2) + R'(\partial V'/\partial t) + V'/C' = V'_{IN}/C' \quad (1)$$

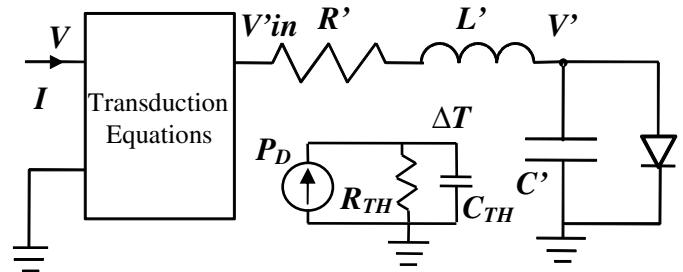


Fig. 1. Compact multiphysics RF large-signal model for an electrostatically actuated MEMS capacitive shunt switch showing the equivalent circuit used to simulate the switch movement. The model is coded in Verilog-A for portability between popular circuit design environments.

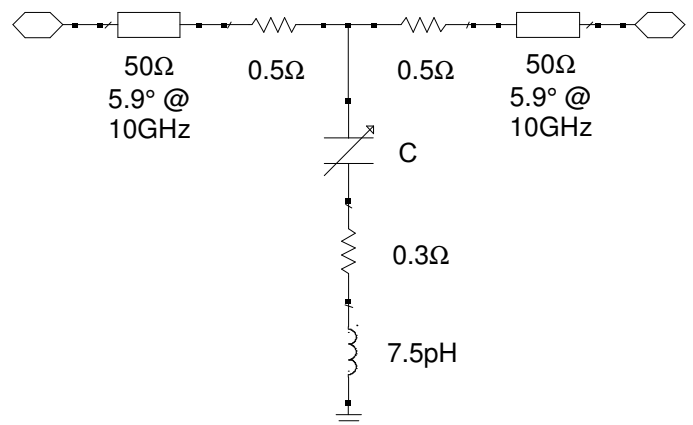


Fig. 2. Complete switch model after adding linear parasitic elements to the nonlinear switch capacitance $C(V)$.

where $L' = m$, $R' = b$, $C' = 1/k$, $V'_{IN} = F/k$, and $V' = z$ represents the average displacement of the membrane from its resting position. Under the parallel-plate approximation, the force F can be described as

$$F \approx \epsilon_0 A V^2 / \left\{ 2 \left[\left(\frac{d}{\epsilon_R} \right) + g - z \right]^2 \right\} \quad (2)$$

where ϵ_0 is the permittivity of vacuum, A , V and g are the overlap, bias and resting ($V = 0$) gap, respectively, between the membrane and the stationary electrode, and d and ϵ_R are the thickness and dielectric constant, respectively, of the insulator on the stationary electrode. Since the present model is coded in Verilog-A, transduction equations such as (2) can be readily implemented to convert V to F . F is then divided by

TABLE I
MODEL PARAMETERS AND THEIR EXTRACTED VALUES

Symbol	Description	Value
m	membrane mass	22 pg
k_0	spring constant	16 N/m
XKT	temperature coefficient of k	0.014 /K
b	damping factor	10 $\mu\text{N}\cdot\text{s}/\text{m}$
A	overlap area	80 $\mu\text{m} \times 120 \mu\text{m}$
d	dielectric thickness	0.25 μm
ϵ_R	dielectric constant	5.0
g	average air gap	2.0 μm
Δg	surface roughness	0.3 μm
I_0	diode saturated current	100 pA
n	power factor of α	1.15
β	average fraction of air gap when breaking contact	0.06
γ_M	adjustment factor of m	-0.55
γ_K	adjustment factor of k	-0.5
γ_B	adjustment factor of b	1.2
R_{TH}	thermal resistance	2100 K/W
C_{TH}	thermal capacitance	83 ns \cdot W/K

k to arrive at V'_{IN} for (1). Solving (1) for V' or z , the switch capacitance C can be evaluated according to

$$C = \epsilon_0 A / [(d/\epsilon_R) + g - z]. \quad (3)$$

To clamp z at g , the capacitor C' is shunted by a diode of a saturated current I_0 and a turn-on voltage $V'_0 = g - \Delta g$, where Δg is the average amplitude of the surface roughness of the stationary electrode.

Fig. 2 shows that based on the nonlinear switch capacitance C , linear parasitic elements due to switch resistance and inductance, as well as input/output transmission-line sections can be added to form a complete switch model. Fig. 2 includes the parasitic element values extracted under small-signal conditions for a typical RF MEMS capacitive shunt switch as described in [14].

Under large RF signals, self heating occurs and the membrane temperature rises above the ambient temperature. Similar to the junction temperature of a transistor, the membrane temperature is some weighted average over a highly nonuniform distribution [16] that can nevertheless account for the self-heating effect globally. Following the approach of transistor modeling, the self-heating effect is captured by a thermal subcircuit with resistance R_{TH} and capacitance C_{TH} so that under steady state

$$\Delta T = P_D R_{TH} \quad (4)$$

where ΔT is the temperature rise and P_D is the dissipated power. As electrostatically actuated MEMS consume hardly any DC bias power, P_D can be evaluated by the RF currents across the three resistors shown in Fig. 2 and verified by subtracting the transmitted and reflected RF powers from the incident RF power.

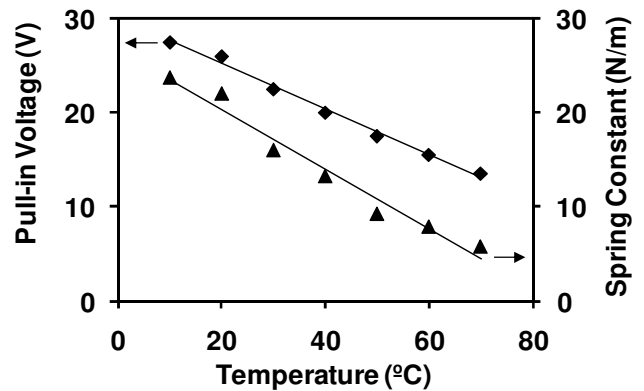


Fig. 3. Measured pull-in voltage (◆) and calculated spring constant (▲) showing linear dependence on ambient temperature.

With increasing temperature, the residual stress of the membrane decreases and its spring constant decreases correspondingly

$$k(\Delta T) = k_0 (1 - XKT \cdot \Delta T) \quad (5)$$

where k_0 is the spring constant at the ambient temperature and XKT is a linear temperature coefficient. If necessary, additional parameters can be made temperature-dependent similar to (5). Table I lists the present model parameters, which includes additional fitting parameters α , β , γ and n for the contact and release processes [14].

III. MODEL VALIDATION

The present model is extracted and validated on state-of-the-art RF MEMS capacitive switches that have been described in detail [17]. Briefly, the membrane is bowtie-shaped and is made of aluminum. The membrane is 120-250 μm wide, 310 μm long and 0.3 μm thick. The stationary gold electrode is 80 μm long and is covered with 0.25 μm of SiO_2 . The small-signal pull-in and release voltages are approximately 25 V and 8 V, respectively. Other material and electrical parameters are listed in Table I.

Similar to the threshold voltage of a transistor, the pull-in voltage V_p of a switch is a critical characteristic and its variations with input power and temperature due to self-biasing and self-heating effects need to be accurately modeled. Fig. 3 shows the measured pull-in voltage of the switch under small signals and different ambient temperatures. From the measured pull-in voltage, the spring constant k and its temperature dependence can be calculated according to [18]

$$V_p = \sqrt{8kg^3/27\epsilon_0 A}. \quad (6)$$

Fig. 3 shows also that the spring constant is linearly dependent on the ambient temperature and its slope corresponds to $XKT = 0.014 /\text{K}$ as listed in Table I.

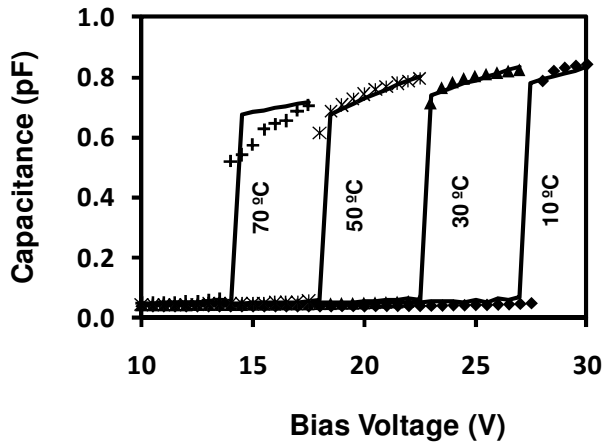


Fig. 4. Measured (symbol) and simulated (curve) capacitance-voltage characteristics both showing that the pull-in voltage decreases with increasing ambient temperature.

The extracted temperature coefficient of the spring constant has been validated through temperature-dependent capacitance-voltage characteristics of the switch as shown in Fig. 4. It can be seen that the present model correctly predicts 1) the shift of the pull-in voltage as a function of ambient temperature, 2) the gradual saturation of the on-capacitance when the bias voltage exceeds the pull-in voltage leading to more intimate contact between the membrane and the stationary electrode, and 3) the decrease of saturated on-capacitance with increasing temperature because although the membrane can be pulled in with lower voltages at higher temperatures, the contact is less intimate under lower voltages. The model cannot predict the sluggish saturation of the on-capacitance at 70°C, because the switch has reached its limit of operating temperature or usefulness.

Due to the highly nonuniform distribution of RF current across the membrane [16], the thermal resistance R_{TH} can be extracted under large signals only. Fig. 5 shows the pull-in voltage measured under a fixed ambient temperature of 25°C but different dissipated RF powers at 15 GHz. Based on the measured pull-in voltage, the membrane temperature can be inferred from the temperature dependence of the small-signal pull-in voltage shown in Fig. 3. Fig. 5 shows also that the inferred membrane temperature is linearly dependent on the dissipated power and its slope corresponds to a thermal resistance R_{TH} of approximately 2000 K/W. Such a large thermal resistance reflects the highly nonuniform current and temperature distributions and is consistent with previous observations [15]. Similarly, the thermal time constant was previously extracted to be 150 μ s, which corresponds to a thermal capacitance C_{TH} of approximately 80 ns·W/K.

Once the thermal resistance and temperature coefficient are extracted, the present model can be used to simulate RF large-signal characteristics. Fig. 6 compares the measured and simulated switch output power vs. the bias voltage under

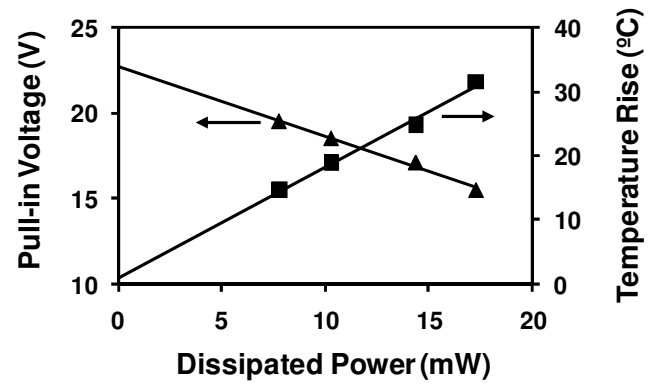


Fig. 5. Measured pull-in voltage (▲) and temperature rise (■) showing linear dependence on the dissipated power at 15 GHz and 25°C.

different input powers at 15 GHz and 25°C. Since the input power is constant while the bias voltage is swept, the test can be regarded as a hot-switching test. The voltage sweep rate, at 1 V/ms, is much slower than either the mechanical or thermal time constant, so the test can be regarded as a steady-state test. It can be seen in Fig. 6 that because the coupled self-biasing and self-heating effects increase with increasing RF power above 20 dBm, the pull-in voltage decreases while the switching becomes less abrupt. These trends are correctly simulated by the model. When the input power is increased beyond 30 dBm, no abrupt change in output power can be observed and the switch becomes a varactor. Thus, the present switch can be considered to have a maximum hot-switching power-handling capacity of approximately 30 dBm.

For more stringent definition of power-handling capacity, Fig. 7 plots the pull-in voltage of Fig. 6 as a function of the input power. It shows that the pull-in voltage decreases linearly with increasing input power as predicted by physical analysis [15]. For certain applications, the power-handling capacity may be defined as the power level under which the pull-in voltage decreases by 10% or 20% from its small-signal value. By being able to predict the slope of the decrease in pull-in voltage with increasing power, the present model can predict at which power level the pull-in voltage will decrease by a given percentage.

IV. CONCLUSION

A compact RF large-signal model was proposed for electrostatically actuated MEMS capacitive shunt switches, which includes not only electromechanical, but also electrothermal and thermomechanical effects. This multiphysics model was validated with measurement of the shift in pull-in voltage over temperature and RF input power. The model could be used to predict RF power-handling capacity under different tests and definitions. The model was implemented in Verilog-A so that it could be easily enhanced and ported to a variety of circuit simulators.

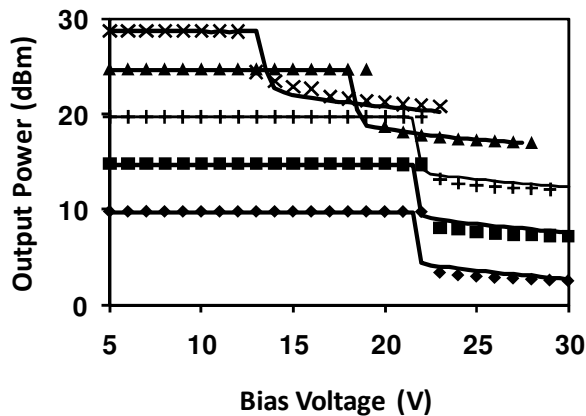


Fig. 6. Measured (symbol) vs. simulated (curve) output power as functions of bias voltage and RF input powers of 10 (◆), 15 (■), 20 (+) 25 (▲) and 29 (×) dBm at 15 GHz and 25°C.

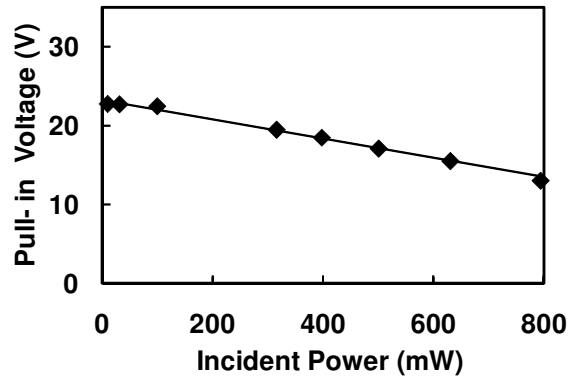


Fig. 7. Measured (symbol) vs. simulated (line) pull-in voltage as a function of RF input power at 15 GHz and 25°C.

ACKNOWLEDGEMENT

This work was supported in part by the US Air Force Research Laboratory under Contract No. F33615-03-C-7003. The contract was funded by the US Defense Advanced Research Projects Agency under the Harsh Environment, Robust Micromechanical Technology (HERMIT) program. In addition, the work was supported by a grant from the Commonwealth of Pennsylvania, Department of Community and Economy Development, through the Pennsylvania Infrastructure Technology Alliance (PITA).

REFERENCES

- [1] J. C. M. Hwang, and C. L. Goldsmith, "Robust RF MEMS switches and phase shifters for aerospace applications," in *Proc. IEEE Radio-Frequency Integration Technology Symp.*, Dec. 2009, pp. 245-248.
- [2] S. D. Senturia, "Microsystem Design." Norwell, Massachusetts: Kluwer, 2001.
- [3] J. B. Muldavin, and G. M. Rebeiz, "Nonlinear electro-mechanical modeling of MEMS switches," in *IEEE MTT-S Int. Microwave Symp. Dig.*, June 2001, pp. 2119-2122.
- [4] D. Mercier, P. Blondy, D. Cros, and P. Guillon, "An electromechanical model for MEMS switches," in *IEEE MTT-S Int. Microwave Symp. Dig.*, June 2001, pp. 2123-2126.
- [5] L. Dussopt, and G. M. Rebeiz, "Intermodulation distorting and power handling in RF MEMS switches, varactors, and tunable filters," *IEEE Trans. Microwave Theory Techniques*, vol. 51, pp. 1247-1256, Apr. 2003.
- [6] D. A. Czaplewski, C. W. Dyck, H. Sumali, J. E. Massad, J. D. Koppers, I. Reines, W. D. Cowan, and C. P. Tigges, "A soft-landing waveform for actuation of a single-pole single-throw ohmic RF MEMS switch," *IEEE J. Microelectromechanical Systems*, vol. 15, pp. 1586-1594, Dec. 2006.
- [7] Z. J. Guo, N. E. McGruer, and G. G. Adams, "Modeling, simulation and measurement of the dynamic performance of an ohmic contact, electrostatically actuated RF MEMS switch," *J. Micromechanics Microengineering*, vol. 17, pp. 1899-1909, Aug. 2007.
- [8] J. Bielen, J. Stulemeijer, D. Ganjoo, D. Ostergaard, and S. Noijen, "Fluid-electrostatic-mechanical modeling of the dynamic response of

- RF-MEMS capacitive switches," in *Dig. Int. Conf. Thermal Mechanical Multi-physics Simulation Experiments Microelectronics Micro-systems*, Apr. 2008, pp. 1-8.
- [9] E. K. Chan, E. C. Kan, R. W. Dutton, and P. M. Pinsky, "Nonlinear dynamic modeling of micromachined microwave switches," in *IEEE MTT-S Int. Microwave Symp. Dig.*, June 1997, pp. 1511-1514.
- [10] G. Bartolucci, R. Marcelli, S. Catoni, B. Margesin, F. Giacomozzi, A. Lucibello, V. Mulloni, and P. Farinelli, "Circuitual modelling of shunt capacitive RF MEMS switches," in *Proc. European Microwave Integrated Circuits Conf.*, Oct. 2008, pp. 362-365.
- [11] E. Lourandakis, G. Fischer, and R. Weigel, "Characterization and modeling of continuously tunable MEMS varactor," in *Proc. German Microwave Conf.*, Mar. 2009, pp. 1-4.
- [12] R. Marcelli, A. Lucibello, G. De Angelis, E. Proietti, and D. Comastri, "Mechanical modelling of capacitive RF MEMS shunt switches" in *Proc. Symp. Design Test Integration Packaging MEMS/MOEMS*, Apr. 2009, pp. 19-22.
- [13] V. Puyal, D. Dragomirescu, C. Villeneuve, J. Ruan, P. Pons, and R. Plana, "Frequency scalable model for MEMS capacitive shunt switches at millimeter-wave frequencies" *IEEE Trans. Microwave Theory Techniques*, vol. 57, pp. 2824-2833, Nov. 2009.
- [14] S. Halder, C. Palego, Z. Peng, J. C. M. Hwang, D. I. Forehand, and C. L. Goldsmith, "Compact RF model for transient characteristics of MEMS capacitive switches," *IEEE Trans. Microwave Theory Techniques*, vol. 57, pp. 237-242, Jan. 2009.
- [15] C. Palego, J. Deng, Z. Peng, S. Halder, J. C. M. Hwang, D. I. Forehand, D. Scarbrough, C. L. Goldsmith, I. Johnston, S. K. Sampath, and A. Datta, "Robustness of RF MEMS capacitive switches with molybdenum membranes," *IEEE Trans. Microwave Theory Techniques*, vol. 57, pp. 3262-3269, Dec. 2009.
- [16] J. B. Rizk, E. Chaiban, and G. M. Rebeiz, "Steady state thermal analysis and high-power reliability considerations of RF MEMS capacitive switches," in *IEEE MTT-S Int. Microwave Symp. Dig.*, June 2002, pp. 239-242.
- [17] C. L. Goldsmith, and D. I. Forehand, "Temperature variation of actuation voltage in capacitive MEMS switches," *IEEE Wireless Components Lett.*, vol. 15, pp. 718-720, Oct. 2005.
- [18] P. M. Osterberg, and S. D. Senturia, "M-TEST: A test chip for MEMS material property measurement using electrostatically actuated test structures," *J. Microelectromechanical Systems*, vol. 6, pp. 107-118, June 1997.